Relativistic modeling for precessing jets: the SS433 X-ray binary environment

Rony Keppens [1,@] , Rémi Monceau-Baroux [1,@] , Oliver Porth [2,@] , Zakaria Meliani [3,@]

1 : Centre for mathematical Plasma Astrophysics, KU Leuven (CmPA) - ***Website***

Celestijnenlaan 200B 3001 Leuven - Belgium

2 : University of Leeds

Leeds - United Kingdom

3 : Observatoire de Paris - Site de Paris (OP) - ***Website***

Observatoire de Paris

61 Av de l'Observatoire 75014 PARIS - France

We present numerical simulations to complement modern radio observations of the helical jets seen in association with X-ray binary SS433. Adopting a 3D relativistic hydrodynamic model, we go beyond the pure kinematic model frequently used to interpret the radio VLA views, pointing out that the gradual build-up of the full helical jet path naturally results in a somewhat decelerated propagation. Synthetic radio maps of the simulated, precessing jets confirm the basic scenario of an overdense jet injected at 0.26c, prevailing at the sub-parsec scale distances. Recent extensions to either larger simulated domains, or to closer in regions including time-variable ejection patterns, will be presented.

Subject :	:	oral
Topics	:	Astrophysics
Topics	:	Numerical simulations

Relativistic modeling for precessing jets:

the SS433 X-ray binary environment

Rony Keppens

Centre for mathematical Plasma-Astrophysics
Department of Mathematics, KU Leuven

with R. Monceau-Baroux, O.Porth and Z. Meliani

XRB SS433

- X-ray binary: AGN jet analogue at smaller scale & in fast-forward: archetype system: SS433 at 5.5 kpc distance
  $\Rightarrow$ giant star [order $\mathcal{O}(10-30M_\odot)$], black hole ($16M_\odot$ Blundell et al. 2008), 13 day binary period

- microquasar XRB system SS433: observed down to sub-parsec scale! mildly relativistic speeds

  $\Rightarrow$ VLA scale (order 0.1 pc) [Blundell & Bowler, NRAO]

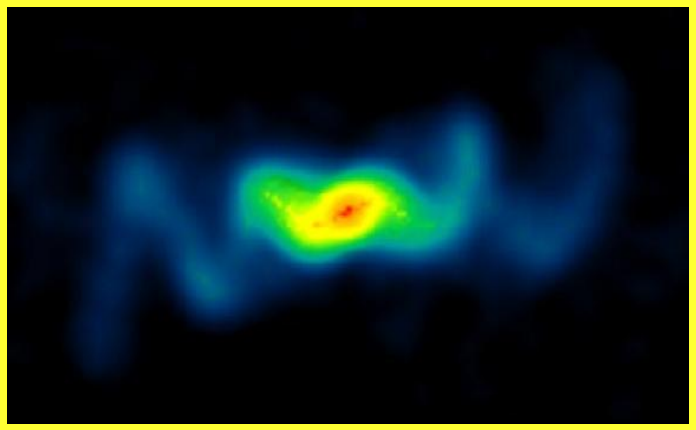

- down to VLBA scale ($\sim$ 0.026 pc), individual blobs $\sim$ 200 AU

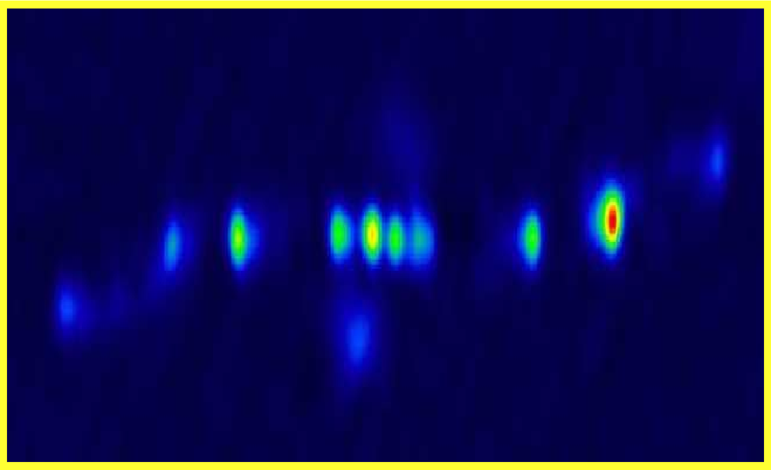

$\Rightarrow$ **SS433 VLBA movie 42 day**

- precessing (+nutation) jet, geometry known, 162 day period!

- artist view shows geometry:

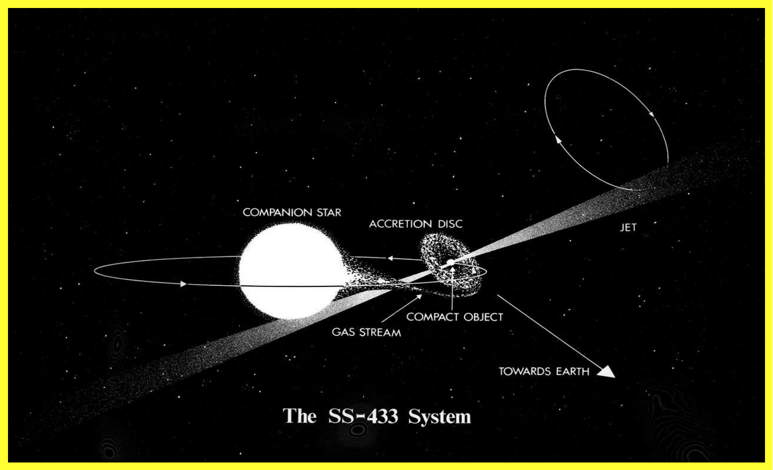

- interacts at larger scales with W50 supernova remnant

Zavala et al. (2008) simulation of SS433

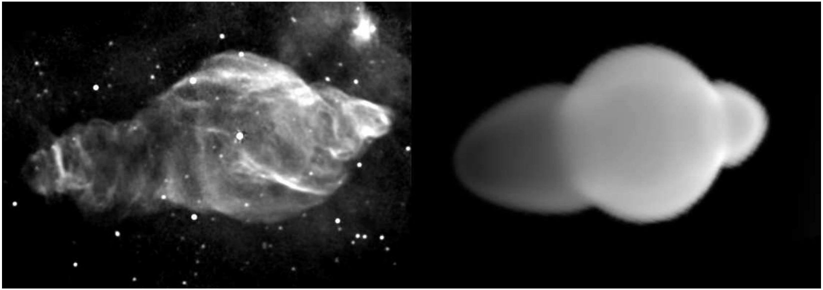

Comparison of the radio-continuum image with the simulated column electronic density map of model M4. The left-hand panel shows the 1415-MHz image in grey-scale and contours of the W50 SNR, obtained with the VLA by Dubner et al. (1998), in equatorial coordinates (north is up). The right-hand panel shows the simulated map in a grey colour scale. A distance of 3 kpc to SS433 was assumed.

Need 10° precessing angle to reproduce the image at 20-50 pc!

Special relativity and (M)HD

- **special relativistic treatment** → flat Minkowski space-time
  - ⇒ particle, tensorial energy-momentum conservation
  - ⇒ use fixed Lorentz frame, 1+3 split (time space), find

$$\partial_t \mathbf{U} + \nabla \cdot \mathbf{F}(\mathbf{U}) = \mathbf{0}$$

  - ⇒ shock-capturing conservative schemes, hyperbolic PDEs
- **MPI-AMRVAC** HTML documentation info at http://homes.esat.kuleuven.be/~keppens
  - ⇒ **Keppens et al, 2012, JCP 231, 741**
  - ⇒ https://gitorious.org/amrvac/amrvac
  - ⇒ develop **Porth**, **Xia**, Meliani, van Marle, vd Holst, RK, ...
- here: **relativistic HD for XRB jet propagation**

Special relativity and (M)HD

- **special relativistic treatment** $\rightarrow$ flat Minkowski space-time
  - $\Rightarrow$ particle, tensorial energy-momentum conservation
  - $\Rightarrow$ use fixed Lorentz frame, 1+3 split (time space), find

$$\partial_t \mathbf{U} + \nabla \cdot \mathbf{F}(\mathbf{U}) = \mathbf{0}$$

  - $\Rightarrow$ shock-capturing conservative schemes, hyperbolic PDEs
- **MPI-AMRVAC** `HTML` documentation info at `http://homes.esat.kuleuven.be/~keppens`
  - $\Rightarrow$ **Keppens et al, 2012, JCP 231, 741**
  - $\Rightarrow$ `https://gitorious.org/amrvac/amrvac`
  - $\Rightarrow$ develop **Porth**, **Xia**, Meliani, van Marle, vd Holst, RK, ...
- here: **relativistic HD for XRB jet propagation**

Quadtree-Octree AMR

- example 2D domain covered by $8 = 4 \times 2$ base level grid blocks
  - $\Rightarrow$ **hierarchically nested** AMR levels, **proper nesting**
  - $\Rightarrow$ fixed **factor** 2 **refinement**

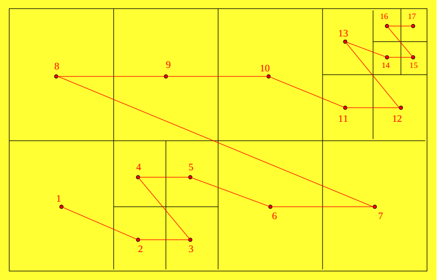

- **Space-filling Morton** (Z-order) **curve**
  - $\Rightarrow$ default: **every timestep full grid-tree re-evaluated**

MPI-AMRVAC and HPC-Europa2

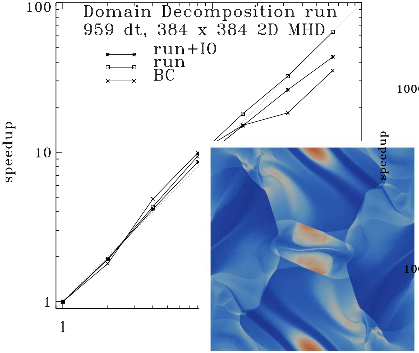

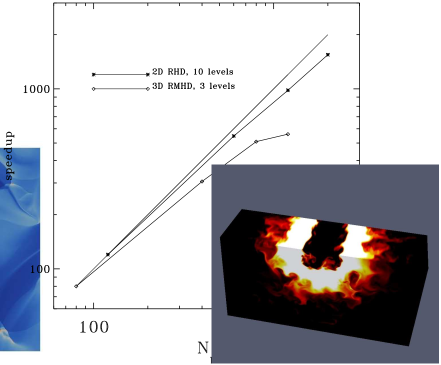

- **excellent scaling**: domain decomposition and **multi-level AMR**
  - $\Rightarrow$ 2D MHD at $\simeq 400^2$, 1000 Δt in $<$ 5 seconds (include IO)
  - $\Rightarrow$ **10 level AMR special relativistic HD sustained 80% efficiency on 2000 CPUs!**

- weak/strong scaling, with(out) AMR, several 1000-10000 CPUs

  ⇒ see **Porth et al, 2014, ApJS, 214, 4**

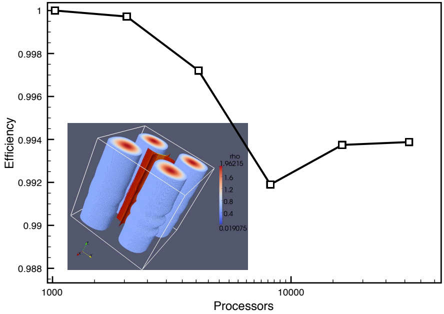

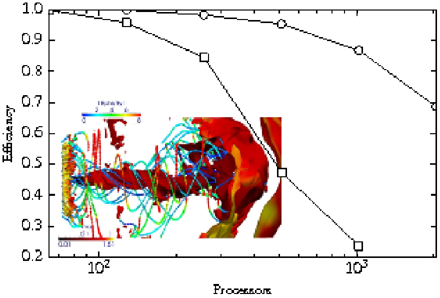

- weak/strong scaling, with(out) AMR, several 1000-10000 CPUs
  ⇒ see **Porth et al, 2014, ApJS, 214, 4**

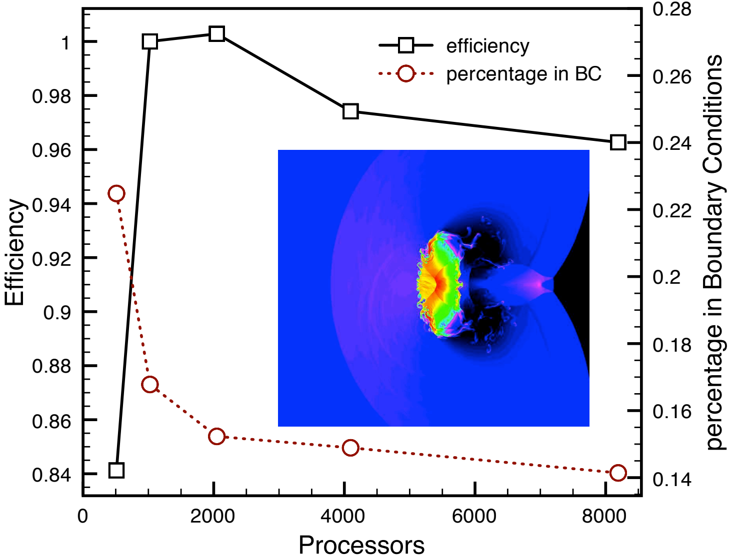

Discretizations and code features

- **shock-capturing schemes, finite volume approach**

  $\Rightarrow$ from TVDLF (used for any system) to more advanced schemes (HLL, HLLC, hybrid HLLC-TVDLF, Roe) incorporating better approximations to the local Riemann fans at cell interfaces
- limited reconstruction (higher order: Koren, Cada, MP5, PPM)

  $\Rightarrow$ **different discretization possible per grid level!**
- active-passive grid blocks; collapse/slice tree during runtime
- extensions to higher order **conservative Finite Differences**

  $\Rightarrow$ see **Porth et al, 2014, ApJS, 214, 4**

- modern applications: circumstellar/binary environments
  - ⇒ Euler + optically thin radiative loss (van Marle et al. 2011)

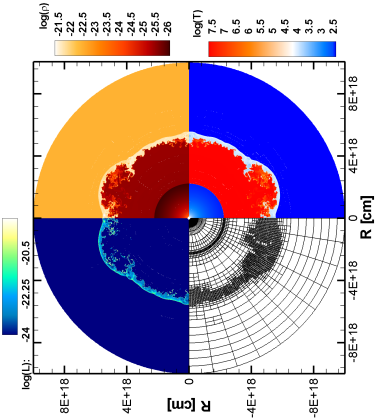

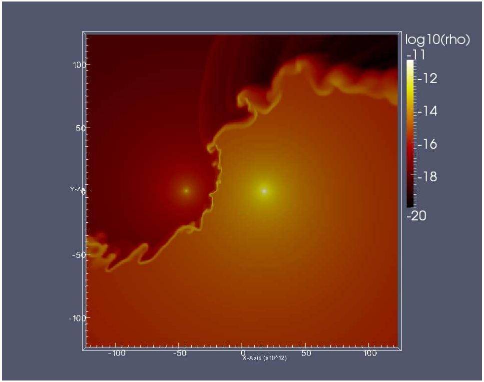

⇒ **3D evolution of orbiting LBV/O stars**

SS433 jet simulations

Aims for the study of X-ray binary associated jets:

1. Better understandings of relativistic jets:
   1. How does precession affect jet/medium interactions?
   2. How do jet properties (v_b/density ratio) affect the interactions?
2. Comparison to observations, in case of SS433 with VLA
   1. synthetic radio (synchrotron) emission maps
   2. compare models in virtual radio views

Geometry

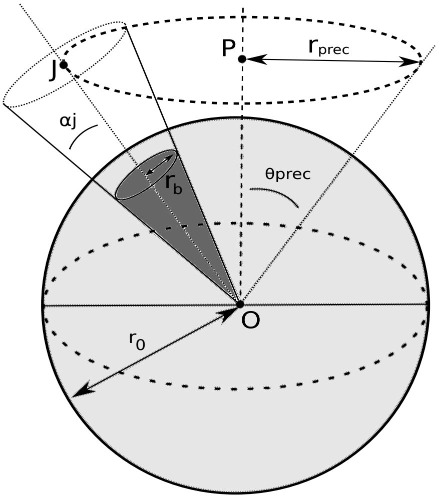

1. Binary system not in model
2. Precessing jet ‘inlet’
3. Overwrite central region
4. two-sided jet

What we know ...

Our input parameters are coming from different observations:

1. The thermodynamic conditions of the ISM, pressure and density: P_{ISM}, ρ_{ISM} (Safi-Harb Oegelman 1997)
2. The energy flux of the jet, $L_j = 10^{39}\,\mathrm{erg\,s}^{-1}$ (Brinkmann et al 2005)
3. The jet opening angle and the jet angle to its precession axis: α_j, θ_{prec} (Margon et al. 1979)
4. The velocity of the jet head: v_{head} (Roberts et al 2008)

... and what we do not!

We fix

1. The jet Lorentz factor, γ_j,
2. $P_j = P_{ISM}$,

... and what we do not!

We need

1. **The jet density, ρ_j.**

As in Meliani et al 2008 and Monceau et al 2012, use integrated energy flux over the beam cross section

$$L_j = (\gamma_j h_j - 1)\rho_j \gamma_j \pi R_j^2 v_j$$

where ρ_j, R_j, v_j are the jet density, radius and velocity. $\rho_j h_j = \rho_j + \frac{\Gamma}{\Gamma - 1} P_j$ is the enthalpy. We can then obtain ρ_j.

4 cases for a global picture

Case	γ_b (v_b)	η	$\theta_{\rm prec}$
A	1.036 (0.26c)	28.6	20°
B	1.87 (0.845c)	0.8	20°
C	1.036 (0.26c)	28.6	10°
D	1.87 (0.845c)	0.8	0°

Tabel: Parameters for the simulations. With $\eta = \gamma_j^2 \frac{\rho_j h_j}{\rho_{ISM} h_{ISM}}$ the inertia ratio.

Let’s have a look

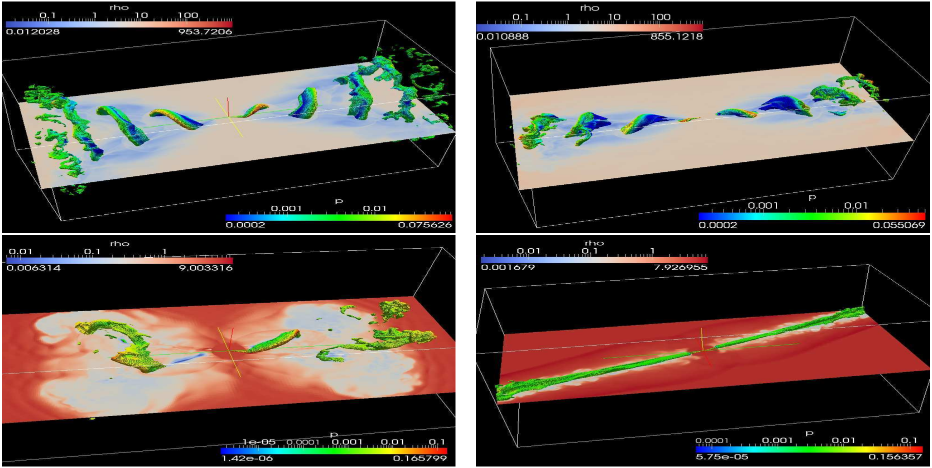

Top: case A, $\gamma = 1.036$ and $t = 2$
Bottom: case B, $\gamma = 1.87$ and $t = 2$

Top: case C, $\gamma = 1.036$ and $t = 2$
Bottom: case D, $\gamma = 1.87$ and $t = 0.5$

- use of (instantaneous and comparative; involve tracer) filters to quantify regions: jet beam, cocoon, SISM, . . . : in cross-section

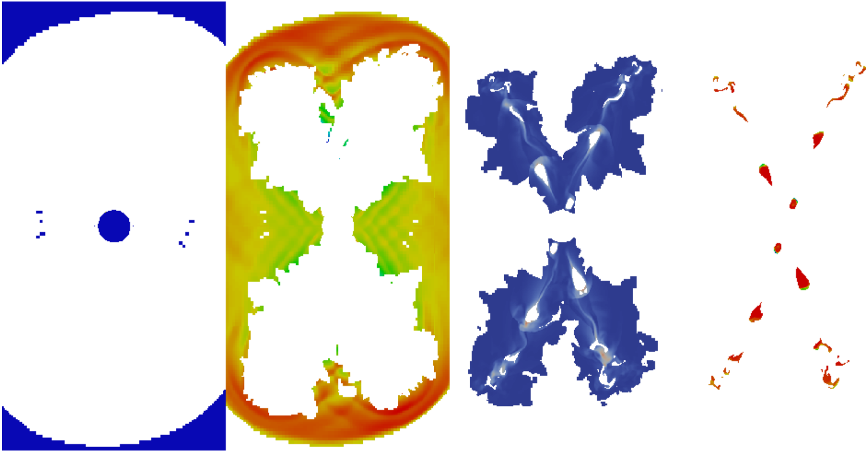

Case D - Overview

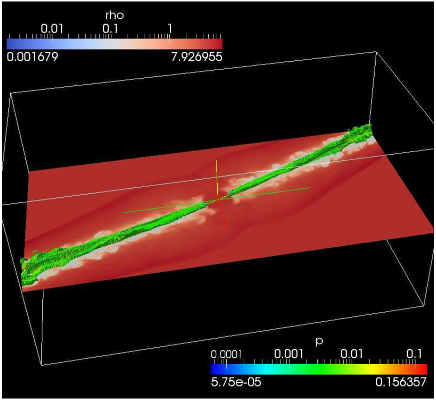

1. 'classic' non-precessing case
2. $\gamma = 1.87$, mildly relativistic
3. Bullet like propagation, canonical relativistic jet behavior (AGN/XRB analogy)

Case D - Dynamics

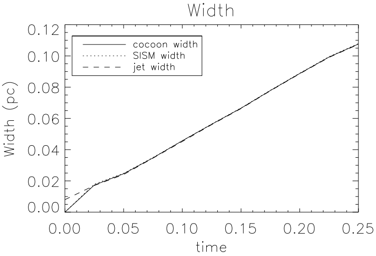

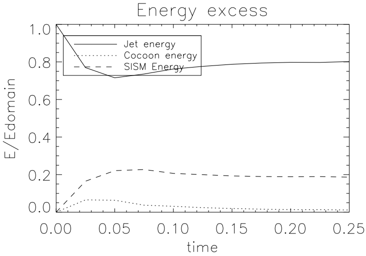

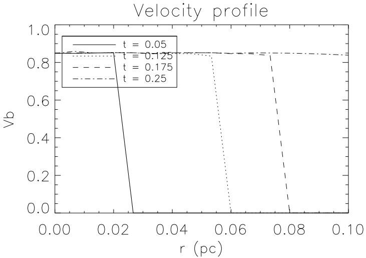

1. propagates with $v_j^{marti} = \frac{\sqrt{\eta}}{\sqrt{\eta}+1} v_{beam}$ with $\eta = \gamma_j^2 \frac{\rho_j h_j}{\rho_{ISM} h_{ISM}}$
2. 'Near' flat velocity profile: only interaction at the head
3. Most energy in the jet beam: low interaction with the medium (low η)

Case D - internal structure: zoomed views

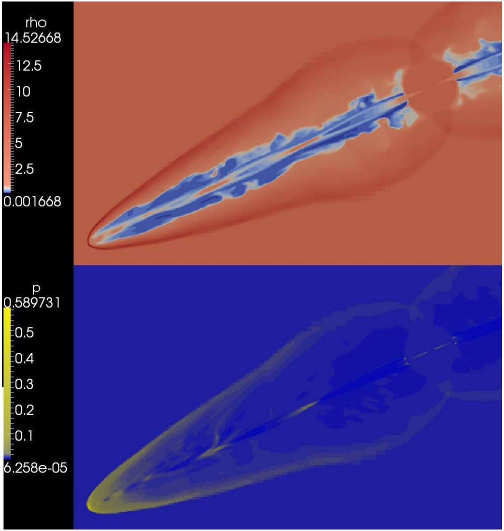

1. Recollimation shocks
2. Structured beam; cocoon & bow shock
3. Instabilities advect down from working surface (Mach disk)

Case B - Overview

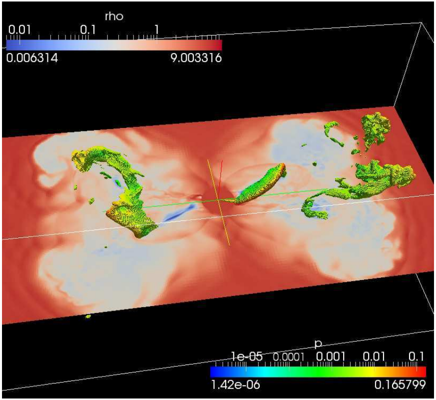

1. Precessing jet
2. Mildly relativistic
3. $\gamma = 1.87$, $\theta = 20^\circ$

Case B - Dynamics

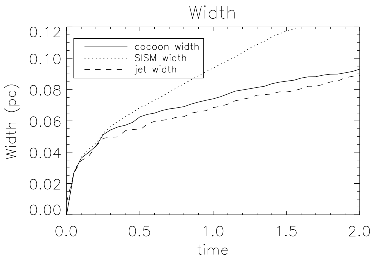

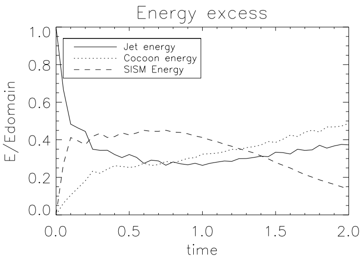

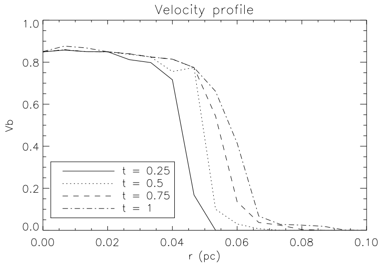

1. Deceleration of jet head velocity to asymptotic regime, sub-sonic velocity of jet head
2. Continuous deceleration along beam path: knee and ankle in velocity profile
3. 30% energy transferred to cocoon and 40% to the SISM

Effect of precession - case B and D

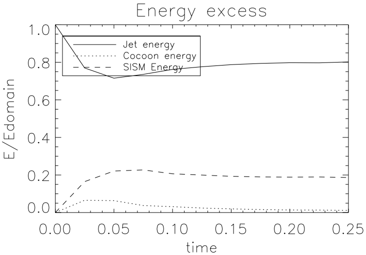

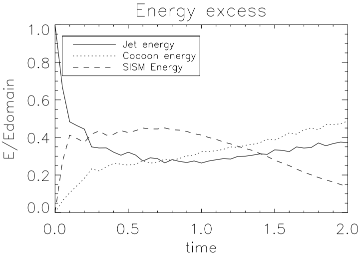

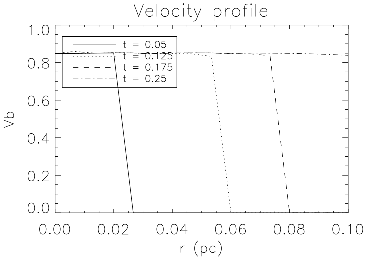

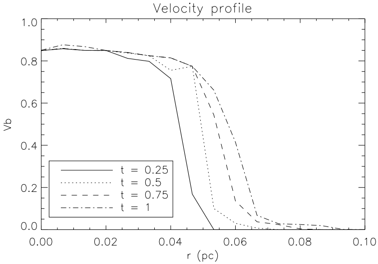

Case A - Overview

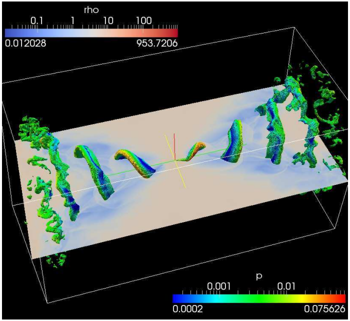

1. Canonical SS433 'kinematic model'
2. Barely relativistic: $\gamma = 1.036$, $\theta = 20^\circ$
3. overdense, canonical jet speed: jet/ISM interaction causes slow-down

- takes longer to build up various windings of helix than estimated from precession/speed

$\Rightarrow$ **ss433 jet buildup**

$\Rightarrow$ **ss433 density in cross-section**

Case A - Dynamics

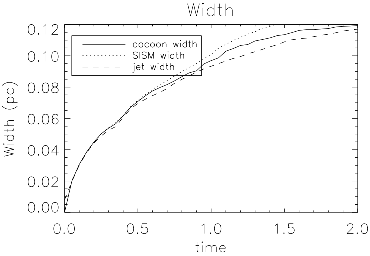

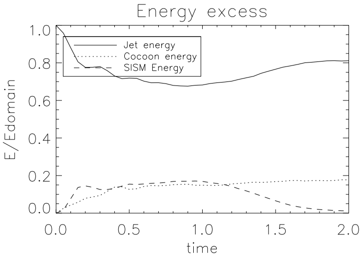

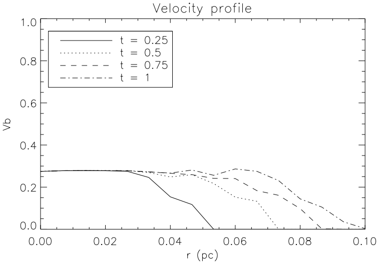

1. Deceleration of jet head velocity, sub-sonic
2. Continuous deceleration along beam path
3. 40% energy transfer to cocoon and SISM

Effect of Lorentz factor - case A and B

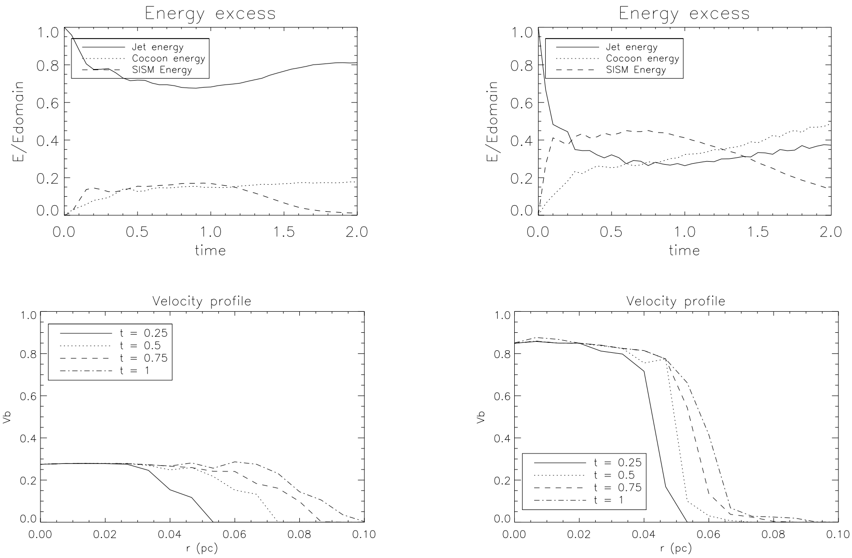

Conclusion on dynamics

1. Case D shows formation of structured beam and inner beam recollimation/standing shocks known from studies of relativistic jets. It interacts weakly with the medium.
2. Precessing cases where a clear shock propagates in front of jet head: velocity profile displays a knee and ankle velocity profile, increased beam-(S)ISM interaction occurs all along jet path. Clear difference in under/overdense cases.
3. Precession increases surface of interaction and energy transfer

Radio Mapping

- Python script for ray tracing through AMR tree/radio mapping [O. Porth]
- Follow energetic electron population density ρ_e along with its passive advection from inlet (ρ_{e0}) where energy spectrum is $f(\epsilon) = A\epsilon^{-\Gamma}$ for $\epsilon \leq \epsilon_\infty$, with $\Gamma = 0.6$.
- Also evolve cut-off energy ϵ_∞, only account for adiabatic losses
- Ray tracing: use emission equation from Camus et al (2009).

$$I = \rho_{e0} \left(\frac{\nu_{obs}}{\nu} \right)^2 B_\perp \left(\frac{\rho_{e0}}{\rho_e} \right)^{-\frac{\Gamma+2}{3}} \epsilon^{1-\Gamma} \left(1 - \frac{\epsilon}{\epsilon_\infty}\right)^{\Gamma-2}, \quad (1)$$

where $\nu \propto B_\perp \epsilon^2$, and $B_\perp$ is the component of the magnetic field normal to the line of sight in the fluid frame and ν_{obs}/ν is Doppler factor.

- hydro result: $B_\perp$ taken proportional to $\sqrt{p}$

Case D - Radio contours

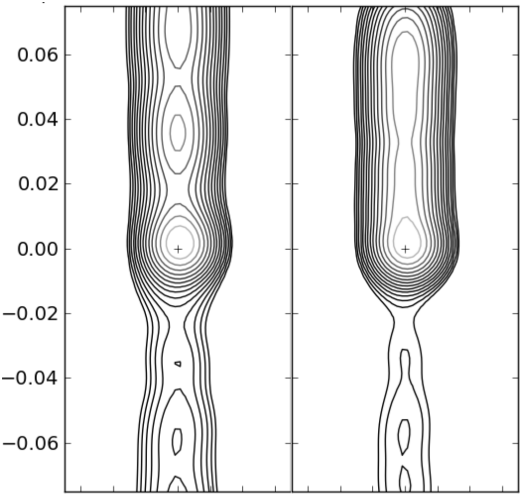

1. Clear appearance of recollimation shocks
2. Strong beaming and line of sight (85° to 78°) effects

Case C - Overview

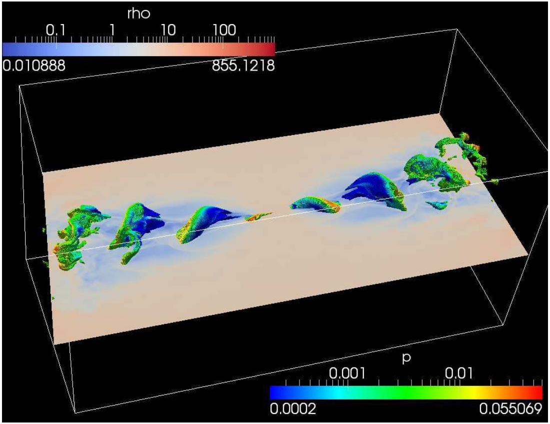

1. Barely relativistic
2. $\gamma = 1.036$, $\theta = 10^\circ$
3. **jet buildup**

Radio mapping - Overview

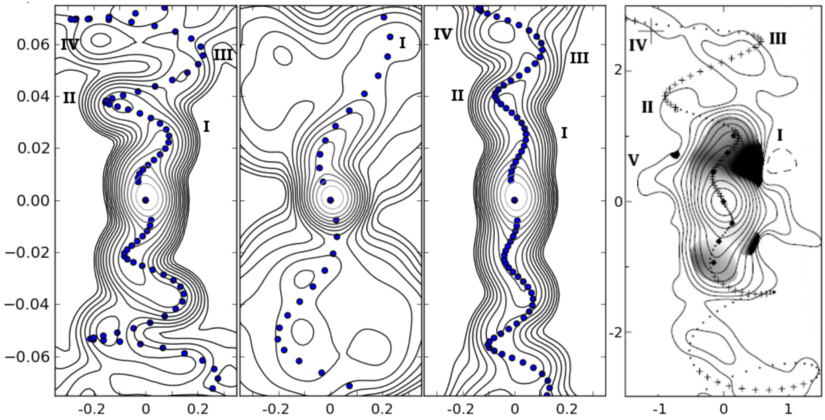

Left to right: Radio map from simulations Case A, Case B and case C. Units are in parsec, object is estimated to be at a distance of 5.5 kpc. All graphs overplot the kinematic model with parameters corresponding to the case. Right: VLA image of the microquasar SS433 in the constellation Aquila, adapted from Roberts et al. 2008, units are in arcsecond.

Case B - Too far

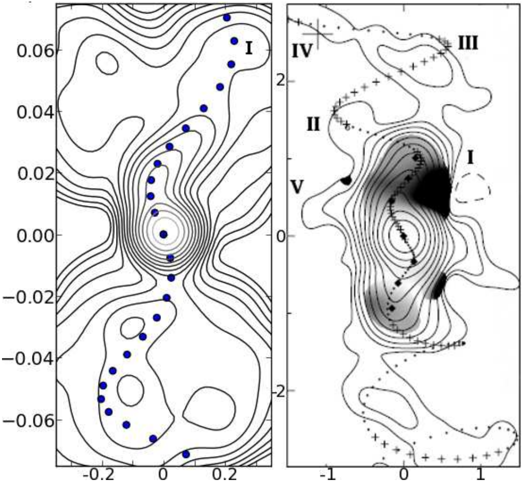

1. Radio elements too far from the source
2. Strong beaming effect

Case C - Too narrow

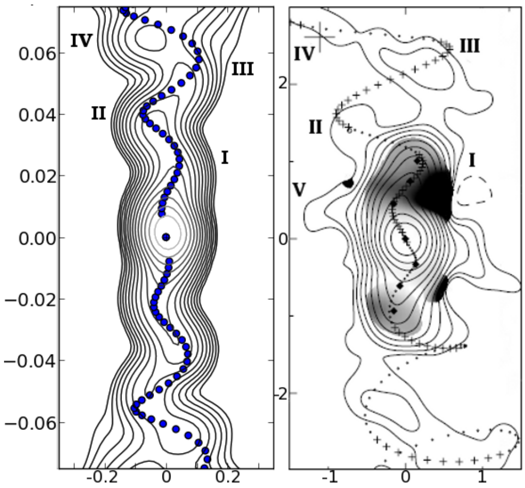

1. Radio elements too close to the precession axis.
2. Different precessing angle with time?

Case A - Good fit

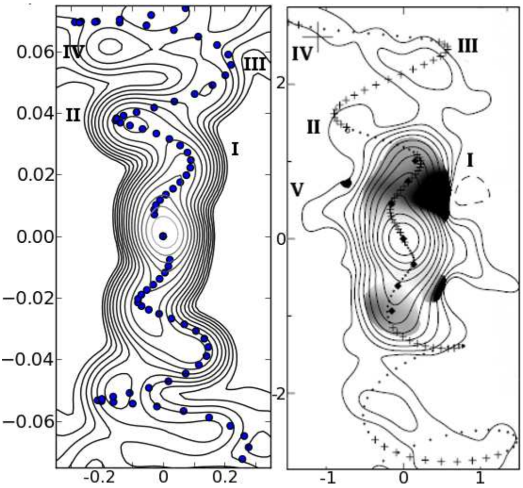

1. Similar appearance
2. kinematic model underestimates interactions for both simulations and observations
3. Absence of radio ruff

Conclusion on dynamics

1. Discrepancy at sub parsec scale and 20 parsec: time variation of the precessing angle? Recollimation?
2. Validation of the kinematic model for SS433. Only case A opening angle and Lorentz factor gives similar picture to VLA observation.
3. The kinematic model needs to be corrected for interactions. It overestimates both simulations and observations.
4. Absence of the radio ruff: are they coming from the disk wind?

Wait a minute!

We have a problem:

1. Small scale (under parsec): 20°
2. Large scale (over 30 parsec): 10°

- Case A at much increased boxsize/keep local resolving power

  $\Rightarrow$ 7 AMR levels, effective $9216 \times 4608 \times 4608$

  $\Rightarrow$ follow from subparsec (beam width size) to parsec scale

Spatial Evolution: 7-11-16-30 years

Use ray-traced $\gamma n_e v \sqrt{p}$ emission proxy

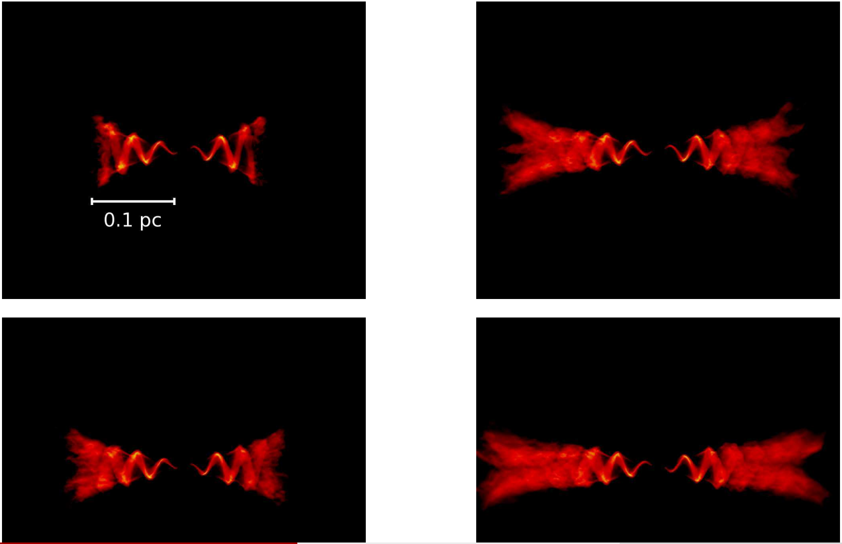

Recollimation

- dynamical recollimation at $\simeq 0.07$ pc where ram and ISM pressure balance

  $\Rightarrow$ evolution of stand-off distance to precession axis

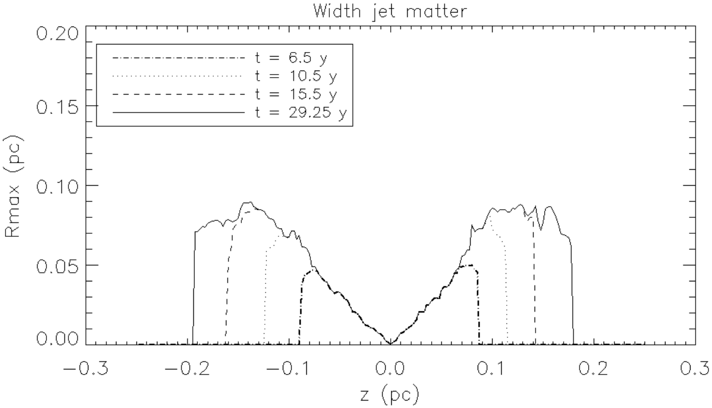

Recollimation

- dynamical recollimation at $\simeq$ 0.07 pc where ram and ISM pressure balance

  $\Rightarrow$ final stand-off location of beam: 20° to $\pm$10° change

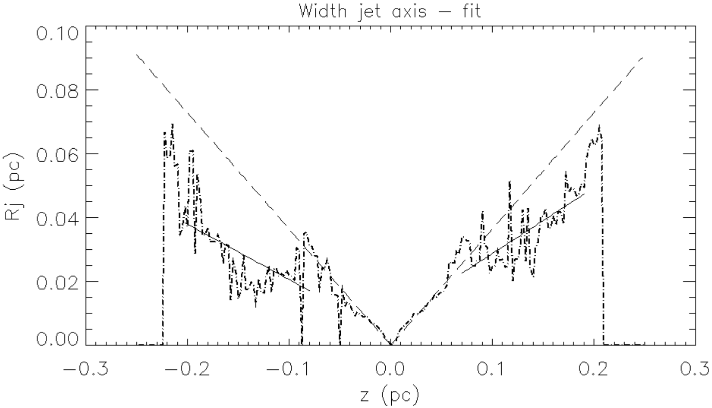

- order pc scale changeover: below VLA sensitivity? Radio map:

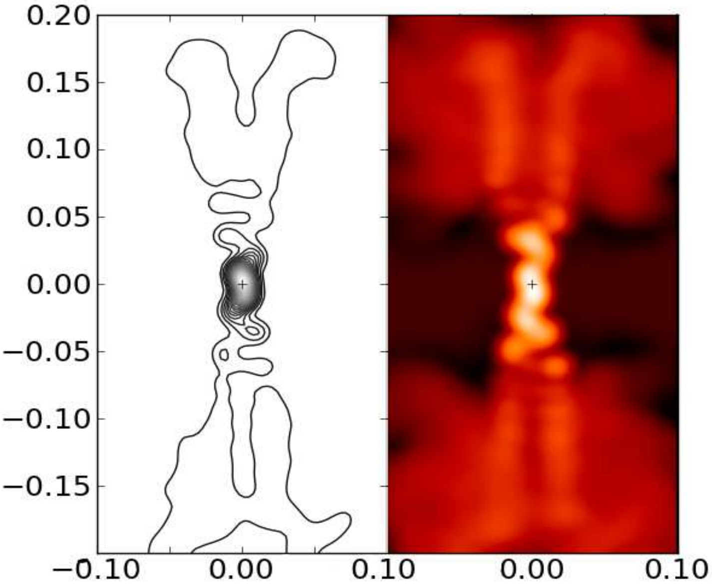

Summary and outlook

- 3D relativistic HD models for precessing jets
  - $\Rightarrow$ quantify energy transfer for up to mildly relativistic cases
- canonical model for SS433 confirmed through model & synthetic radio observation
  - $\Rightarrow$ Monceau-Baroux et al, 2014: role of deceleration!
- larger-scale follow-up: discovery of dynamical recollimation
  - $\Rightarrow$ ok to use hollow continuous jet model further out!
  - $\Rightarrow$ Monceau-Baroux et al, 2014 (submitted)
- Plans: zoom into VLBA scales (variability)
  - $\Rightarrow$ **model jet progression through disk wind zone**
  - $\Rightarrow$ incorporate magnetic fields, . . .